

## Hydrate slurry rheology in the petroleum industry

Karin Hald & Sven Nuland

Institute for Energy Technology, P.O. Box 40, NO-2027 Kjeller, Norway

### ABSTRACT

Modern methods of controlling hydrate problems in petroleum production involve transport of a dispersion of hydrate particles in oil. This necessitates the determination of the rheological properties of this settling slurry. Methods are discussed and preliminary results given. Means for accounting for the effect of distribution of particles are discussed.

### INTRODUCTION

In the petroleum industry, hydrate formation is a flow assurance problem. Hydrates are ice-like crystals (clathrate) formed by water and gas under pressure and suitably low temperatures that agglomerate and form blockages in production lines. The conditions for hydrate formation are characterized by Pressure-Temperature diagram (PT-diagram) for the concerned gas.

The used hydrate prevention methods are approaching their limits for the deeper and longer production lines. Two common methods are

- Thermal insulation of the parts satisfying the pressure and temperature conditions for hydrate formation from a Pressure-Temperature diagram and,
- Adding Mono-Ethylene Glycol (MEG) in order to move the pressure and temperature conditions for hydrate formation.

These methods involve complex systems to operate and may not be sufficient in the

future (Sloan<sup>3</sup>). Concerning MEG, high concentrations (above 40%) are required, resulting in high operating costs and capacity problems for long transport pipes in deep water.

Now, new methods accepting hydrate formation under controlled conditions are evaluated. One, here investigated, consist of adding small amounts (1.5%) of anti-agglomerates in the pipe such that the surface characteristics of the hydrates changes. In this manner, the hydrates do no longer stick to the wall or to each other but are transported in the fluid as small particles.

However, the phase change from water to hydrates results in the formation of a suspension called “hydrate slurry”. Its characteristics is concentration, particle size distribution, particle density and from a flow assurance point of view, apparent viscosity. Hydrate slurry rheology has been studied earlier in the petroleum field (Camargo et al.<sup>4</sup>, Siquin et al.<sup>5</sup> and Fidel-Dufour et al.<sup>6</sup>) and the refrigeration field (Ayel et al.<sup>7</sup> and Darbouret et al.<sup>8</sup>).

Multiphase flow modelling for the petroleum industry consists in determining the flow properties with respect to the fluids and solids in the pipeline. Since the hydrate formation lead to a viscosity change, this part has to be quantified in order to keep the models updated with this new solution.

Therefore, this work consists of an experimental approach where the viscosity of hydrate slurries is measured with re-

spect to the hydrate concentration. Viscosity and yield stress measurements are performed in a pressure cell of a rheometer with Couette cylinder geometry.

For suspensions, particle migration during measurements leads to under- or over-estimation of the viscosity. In this project, shear induced particle migration is modelled in order to evaluate its influence on the experimental results.

The experimental setup is presented in the following section. Next, results from preliminary tests are given. Then, a model of shear induced particle migration based on Leighton & Acrivos<sup>1</sup> work is given, followed by an evaluation of the experiments, some future plans and finally, the conclusions.

## MATERIAL & METHODS

The experimental procedure consists of the hydrate slurry formation in a stirred reactor, the transfer under constant pressure and temperature conditions to a pressure cell in the rheometer and finally, viscosity measurements. These steps are described in this section.

In a stirred reactor, oil, water, and gas are mixed under appropriate pressure and temperature conditions with respect to the PT-diagram. In the preliminary tests, sulphur-hexafluorid ( $\text{SF}_6$ ) is used as it permits the formation of hydrates at fairly low pressure and temperature. Typically, the pressure and temperature are about 8 bar and 2°C. In addition, 1.5% anti-agglomerate inhibitor is added to the water such that the hydrates do not agglomerate and stay as particles in the oil.

Three concentrations have been tested, 10, 20 and 40%. When the hydrate formation starts, all the water is rapidly converted to hydrates. An example of pressure history during hydrate formation is presented in figure 1. The first pressure drop is due to cooling of the stirred reac-

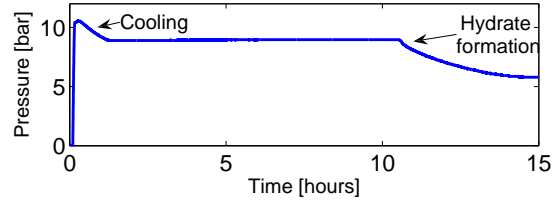


Figure 1. Time history of pressure during hydrate formation

tor, and the second to hydrate formation and the accompanying gas absorption.

The oil, which becomes the carrier fluid after the phase change has a viscosity of 3 mPa.s and a density of 802 kg/m<sup>3</sup>. However, under pressure, the oil absorbs  $\text{SF}_6$  gas and the density has been measured to 825 kg/m<sup>3</sup> at 8 bar which should be considered in this case. The density of the hydrates are estimated to 910 kg/m<sup>3</sup>. In this manner, the difference between the densities is known.

After the fluids are mixed and pressurized, the reactor is cooled with a external cooling cap. The hydrate formation time seems quite random and can take up to several days. It is observed as a pressure decrease in the stirred reactor (see fig. 1). Once the hydrates are formed, samples can be transferred to the rheometer for viscosity measurements.

Before the transfer, the pressure and temperature of the rheometer are set like in the stirred reactor. The transfer is pressure driven, with small differences, and the transfer time is maximum one minute. The transfer of the sample seems to be the factor which leads to the highest uncertainty in the measurement. At low concentrations and long transfer times, separation has been observed during transfer. This change the concentration of the sample in the rheometer since the filling is located in the bottom and the outflow in the top of the geometry. The uncertainty is related to the concentration of the hydrate slurry

in the pressure cell of the rheometer. Attempts to check the concentration after the viscosity measurements by analysing the sample are made, but are not always successful to confirm the concentration; under pressure release, the hydrates decompose and the sample expands and creates foam which is difficult to have under control.

Measurements are performed in a pressure cell, of a Physica MCR301 rheometer from Anton Paar. A Couette cylinder geometry is used with a gap size of 1.055 mm. The hydrates particles have been estimated to be 100-200  $\mu\text{m}$ . The particle to gap size ratio is therefore above 5.

Fig. 2 is a picture of the cooler, the stirred reactor and the rheometer with the pressure cell.



Figure 2. Photography of the experimental facility

Flow curves are achieved by viscosity measurement at different shear rates. The measurement consists of loop tests in the sense that the shear rate is increased, and then decreased, and this loop is performed several times in a row.

The temperature is controlled and datalogged. There is on the actual setup no possibility to datalog the pressure in the rheometer. However this will be done in the future as variations have been observed.

## EXPERIMENTAL RESULTS

In the preliminary tests, the influence of concentration is evaluated by flow curves, in order to define the viscosity and yield stress of the sample.

Figure 3 and 4 presents the flow curves with respect to the viscosity and shear stress respectively. The presented results are mean values from a number of experiments. The variability of the results increase with decreasing shear rate, however, a clear trend is observed, demonstrating the influence of concentration. The measurements fit the Herschel-Bulkley model.

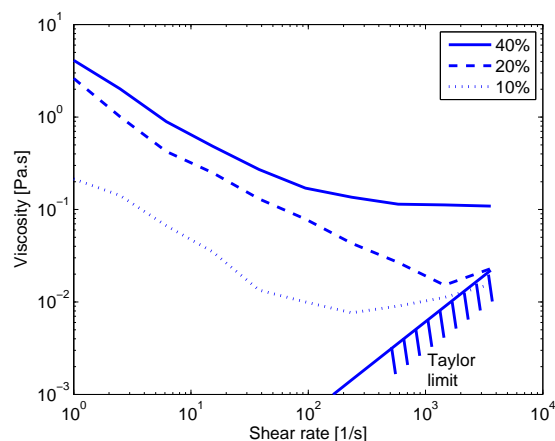


Figure 3. Flow curves for different concentrations

At 40% concentration, the measurements often present high concentration suspension characteristics. Jamming has also occurred during sample transfer. Individual results presents jumps in the flow curves suggesting changes in the particle structure or wall slip as shown in fig. 5.

All measurements present shear thinning behaviour.

For samples containing 10% hydrates, a larger variability of results is found. The uncertainty of the concentration is also higher in these cases due to a more rapid phase separation during transfer.

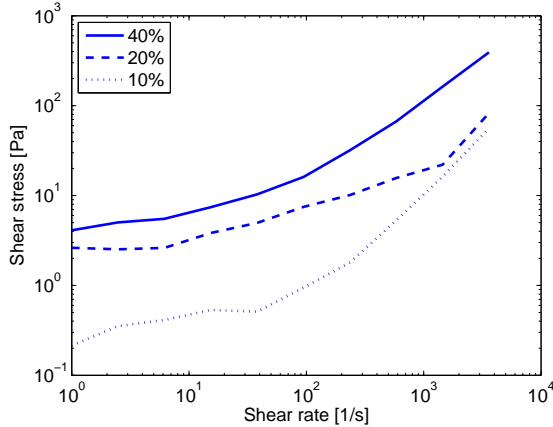


Figure 4. Flow curves for different concentrations

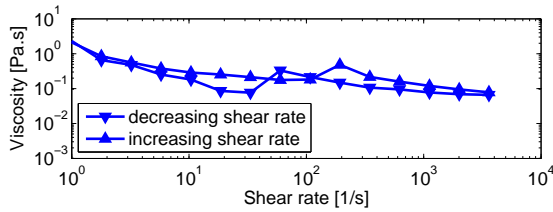


Figure 5. Example of high concentration suspension effects

With 20% hydrate fraction, the slurry presented the most repeatable results. In some cases, an equilibrium loop was measured up to four times in a row on the same sample.

At low concentrations and high shear rates, the measurements reach the Taylor limit. The presented results show as expected an increase in viscosity due to the Taylor vortices in this region.

In figure 6 the temperature history during the viscosity measurement is presented. This measurement started with decreasing shear rate (line), followed by increasing shear rate (dotted line). In both cases, an increase in temperature is observed at high shear rates. This is most probably due to hydrates breaking up, releasing gas and heating the system. The increase is much more pronounced for decreasing shear rates than increasing shear

rates. After, the temperature goes below the setpoint temperature ( $2^{\circ}\text{C}$ ) due to the time response of the cooling device in the rheometer being lower than the measurement time during these points. This part will be further investigated with a pressure transducer on the rheometer, in order to measure the observed but not measured pressure change in the pressure cell.

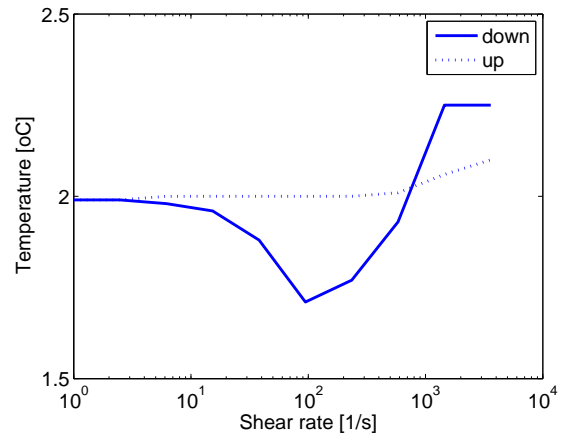


Figure 6. Temperature evolution during the viscosity measurement

## MODELLING PARTICLE MIGRATION

Preliminary observations indicate that the hydrates particles are settling due to gravity. They may also be unevenly distributed in the horizontal direction in the rheometer gap creating wall slip, but we will as a first step concentrate on the effects of gravitational settling.

We will assume a model for the vertical distribution of particles, and a model for the viscosity as a function of particle concentration with unknown parameters. We assume that this viscosity function is valid at each vertical position in the rheometer, with the local particle concentration. We will then try to determine the unknown parameters by minimizing the difference between the measured torque and the one predicted.

A model based on several previous

works is now presented for the case of particle migration described by the shear generated diffusion as described by Leighton & Acrivos<sup>1</sup> balancing gravitational settling and including hindered settling due to particle migration. The particles will tend to accumulate at the bottom while the concentration decreases with height.

For a given mean concentration, a vertical concentration profile is modelled. From this, a viscosity profile will be deduced. Assuming the measured viscosity is a mean of the modelled viscosity profile, they may be compared.

The shear induced particle migration flux is given by

$$J_D = -\dot{\gamma}a^2\hat{D}\frac{d\Phi}{dz} \quad (1)$$

where  $\hat{D} = \frac{1}{3}\Phi^2(1 + \frac{1}{2}\exp 8.8\Phi)$ . The vertical balance between gravitation and shear in the suspension is then

$$\Phi\frac{2}{9}a^2fg\frac{\Delta\rho}{\mu_0} = -\dot{\gamma}a^2\hat{D}\frac{d\Phi}{dz} \quad (2)$$

where the shear rate  $\dot{\gamma}$  is constant and  $f$  is the hindrance to particle settling caused by the presence of other particles in the suspension.

Assuming  $f = (1 - \Phi)^{4.5}$  (Jaisinghani<sup>9</sup>), we get

$$-\frac{2}{3}\frac{g\Delta\rho}{\dot{\gamma}\mu_0}dz = \frac{\hat{D}}{\Phi(1 - \Phi)^{4.5}}d\Phi. \quad (3)$$

This differential equation has to be solved by numerical integration. For a given case, the average concentration is defined by

$$\bar{\Phi} = S \int_0^h \Phi(z)dz / (S \cdot h). \quad (4)$$

For a given mean concentration  $\bar{\Phi}_{meas}$ , we iterate on the bottom concentration  $\Phi_b$  in order to find a distribution that gives  $\bar{\Phi} = \bar{\Phi}_{meas}$  where the boundary condition  $\Phi(z = 0) = \Phi_b$  yields.

Fig. 8 presents the vertical concentration profile for different concentrations. The particle migration increases in distance with the mean concentration of particles. For a given concentration, it increases with the shear rate  $\dot{\gamma}$ .

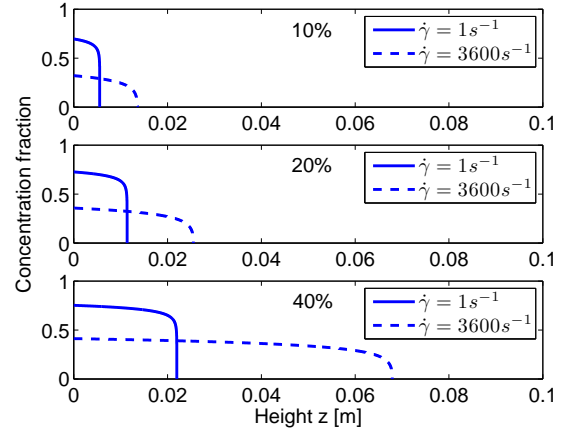


Figure 7. Vertical concentration profile for different mean concentration

Now, a vertical viscosity profile is found through the Krieger-Dougherty model

$$\mu(z) = \frac{\mu_0}{(1 - \frac{\Phi(z)}{\Phi_m})^m} \quad (5)$$

where  $\Phi_m$  is the maximum packing fraction. The shear stress is then given by

$$\tau(z) = \mu(z) \cdot \dot{\gamma} \quad (6)$$

$$\bar{\tau} = S \int_0^h \tau(z)dz / (S \cdot h) \quad (7)$$

where  $S$  is the circumference and  $h$  is the height. The unknown parameters  $m$  and  $\Phi$  are then determined by minimization.

## DISCUSSION

Vertical particle settling due to gravitational effects, can lead to lower or higher than actual viscosity in a Couette geometry. If the settling particles are located in the gap under the cylinder (typically for low concentrations) the measurement will be performed on the carrier liquid and present a lower viscosity. On the other

hand, if one thinks of a high concentration suspension, the lower settled layer will be higher, and may “brake” the cylinder. In this case, the measured viscosity will be higher than the one of the suspension. Fig. 8 illustrates this effect.

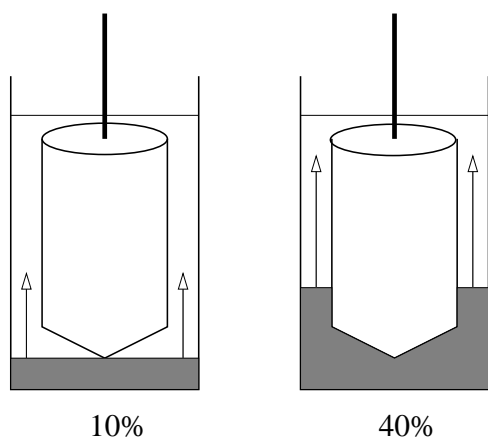


Figure 8. Different concentrations in Couette geometry before resuspension

In fig. 3, a shear thickening behaviour is observed at high shear rates before the Taylor limit. The presented particle migration model suggest an explanation for this behaviour at low concentrations. It might be due to the low concentration, that sedimentate under the cylinder at low shear rates and create a resuspension at higher shear rates that grow to the measurement zone.

The viscosity measurement is performed in the gap between the cylinder and the cup. For small concentration, one can imagine the particles have settled under the cylinder. A resuspension at higher shear rates could then lead to a higher viscosity when particles migrate in the measuring zone.

On the other hand, at high concentrations and high shear rates, the particle concentration in the measuring zone will decrease and result in shear thinning.

## FUTURE PLANS

In the presented results, wall slip and particle migration are observed phenomena. For this reason, different geometries are designed in order to minimize these effect, or at least try to enlarge the measurement regions.

- The first geometry consists of a cylinder in cup geometry, with a roughness on the surfaces. This geometry will be calibrated with standard oil in order to perform viscosity measurements.
- The second is a stirrer geometry, which is appropriate for the measurement of yield stress. It is convenient for suspensions with particle sedimentation.

In addition, particle size distribution measurements are planned to characterize more precisely the particle to gap ratio.

All these measurements will be undertaken in the near future, and results will be presented at NRC2007 at Stavanger in June.

## CONCLUSIONS

The preliminary test of hydrate slurry rheology with sulfur-hexafluorid gave promising results. Of course, some challenges have to be accounted for, as it concerns measurements of suspensions, at that particle migration occur during the measurement.

Anyway, a clear difference between different concentrations is found. Higher concentration results in higher viscosity. Generally, flow curve demonstrate shear thinning behaviour. At low concentrations, the results reach the Taylor limit at high shear rates and the viscosity increases as expected. In addition, shear thickening occur at high shear rate. A possible explanation of resuspension in the measurement region is given. At high concentra-

tion, particle packing presents sometimes jumps in the viscosity measurements.

Temperature history during the measurement shows heating at high shear rates. This suggests hydrate break up. However, this needs to be confirmed by pressure history in the pressure cell of the rheometer.

A model for the balance between gravitation and shear induced particles migration is given. For different concentrations, it demonstrates the sedimentation at low shear rate and resuspension for high shear rate.

#### ACKNOWLEDGEMENTS

The project is conducted at the Institute for Energy Technology in Norway. This work was made possible by financial support from the Norwegian Research Council and HORIZON.

#### REFERENCES

1. Leighton, D. & Acrivos, A. (1986), "Viscous resuspension", *Chemical Engineering Science*, Vol. 41, No. 6.
2. Barnes, H.A. (1997), "Thixotropy - A Review", *J. Non-Newtonian Fluid Mech.*, 70.
3. Sloan, E.D. (2005), "A changing hydrate paradigm - from apprehension to avoidance to risk management", *Fluid Phase Equilibria*, 228-229.
4. Camargo, R., Palermo T., Siquin, A. & Glenat P. (2000), "Rheological Characterization of Hydrate Suspensions in Oil Dominated Systems", *Ann. N.Y. Acad. Sci.*, 912.
5. Siquin, A., Palermo T., & Peysson Y. (2004), "Rheological and Flow Properties of Gas Hydrate Suspensions", *Oil & Gas Science and Technology*, 59.

6. Fidel-Dufour A., Gruy F. & Herri J.-M. (2006), "Rheology of methane hydrate slurries during their crystallization in a water dodecane emulsion under flowing", *Chemical Engineering Science*, 61.

7. Ayel, V., Lottin, O. & Peerhossaini, H. (2003), "Rheology, flow behaviour and heat transfer of ice slurries: a review of the state of the art", *International Journal of Refrigeration*, 26.

8. Darbouret, M., Cournil, M. & Herri, J.-M. (2005), "Rheological study of TBAB hydrate slurries as secondary two-phase refrigerants", *International Journal of Refrigeration*, 28.

9. Jaisinghani, R. A. (1982), "Liquid-Liquid separation", *Handbook of multi-phase systems*, 9:116-146